Available online at www.sciencedirect.com
SCIENCE DIRECT®
Journal of Magnetic Resonance 171 (2004) 143–150
JMR Journal of Magnetic Resonance
www.elsevier.com/locate/jmr

Water suppression without signal loss in HR-MAS ^{1}H NMR of cells and tissues

Jin-Hong Chen[a], Elliot B. Sambol[a], Peter T. Kennealey[a], Rachael B. O'Connor[a], Penelope L. DeCarolis[a], David G. Cory[b], Samuel Singer[a,*]

[a] *Sarcoma Disease Management Program, Memorial Sloan-Kettering Cancer Center, New York, NY 10021, USA*
[b] *Department of Nuclear Engineering, Massachusetts Institute of Technology, Cambridge, MA 02139, USA*

Received 19 July 2004; revised 16 August 2004
Available online 17 September 2004

Abstract

In cell and tissue samples, water is normally three orders of magnitude more abundant than other metabolites. Thus, water suppression is required in the acquisition of NMR spectra to overcome the dynamic range problem and to recover metabolites that overlap with the broad baseline of the strong water resonance. However, the heterogeneous cellular environment often complicates water suppression and the strong coupling of water to membrane lipids interferes with the NMR detection of membrane associated lipid components. The widely used water suppression techniques including presaturation and double pulsed field gradient selective echo result in more than a 70% reduction in membrane associated lipid components in proton spectra of cells and tissues compared to proton spectra acquired in the absence of water suppression. A water suppression technique based on the combination of selective excitation pulses and pulsed field gradients is proposed to use in the acquisition of high resolution MAS NMR spectra of tissue specimens and cell samples. This pulse sequence methodology enables efficient water suppression for intact cells and tissue samples and eliminates signal loss from cellular metabolites.

Keywords: Water suppression; HR-MAS NMR; Presaturation; SEEN

1. Introduction

For the semi-solid samples such as cultured cells or tissues, magic angle spinning (MAS) NMR [1] provides spectra with increased sensitivity and resolution [2–5]. High resolution MAS NMR spectroscopy is now widely used for in vitro and ex vivo studies [2–10]. In the field of cancer research, MAS NMR has been used to: (a) distinguish tumor types using biomolecular markers [2,8,11], (b) characterize malignant potential of certain cancers [10,12], and (c) monitor the response of tumors to chemotherapy and/or radiotherapy [3]. MAS removes the major line-broadening mechanisms in tumor tissue and cell samples, including most of the dipolar coupling and susceptibility inhomogeneity across the sample. However, the heterogeneous features of these natural samples largely remain and compromise the quantitative analysis of the MAS NMR spectra. For example, water interacts strongly with membrane lipids such as phosphatidylcholine but not with some small metabolites such as phosphocholine and free amino acids. In addition, relaxation times of membrane lipid protons are significantly different from the free small metabolites. Accordingly, the design of NMR experiments for HR-MAS NMR analysis of cells and tissues (complex semi-solid systems) must take these factors into account when applying the

* Corresponding author. Fax: 1 646 422 2300.
E-mail address: singers@mskcc.org (S. Singer).

1090-7807/$ - see front matter © 2004 Elsevier Inc. All rights reserved.
doi:10.1016/j.jmr.2004.08.009

existing experimental techniques that have largely been developed for the static NMR studies of liquid systems.

In tissue or cultured cells, water is normally three orders of magnitude more abundant than other metabolites. Thus, water suppression must be applied in the acquisition of high quality NMR spectra to overcome the dynamic range problem and to recover metabolites that overlap the broad baseline of the strong water resonance [13]. Eliminating water without perturbing other resonances is ideal but not realistic. There are three key factors that may define the requirements for water suppression techniques: (i) no other signal loss; (ii) narrow suppression band across the water region in the spectra; and (iii) efficient on-resonance suppression. Requirement (i) may be the most important factor of these three. Large signal loss results in decreased sensitivity and may lead to significant errors in quantitative analysis especially when metabolites are suppressed to unequal degrees. NMR is a technique of inherently low sensitivity. Further signal reduction in experimental design should be avoided particularly when it results in a non-uniform reduction in metabolite signals. The ideal efficiency for water suppression is when the residual water signal is lower than the largest metabolite signal allowing the spectra to be acquired using the largest receiver gain. However, less strict receiver gain requirements are usually necessary for the acquisition time to be practical.

Till today, all of the high-resolution MAS NMR spectra acquired on tissue and cell samples have utilized the presaturation technique [2–12,14], which indeed achieves efficient water suppression and a flat baseline. A selective-gradient-echo, such as the widely used excitation sculpting in liquid NMR experiments [15,16], may be used for water suppression in cell and tissue samples as well. In this paper, we show that both methods fail for tissue and cell samples by significantly reducing the intensities of lipid signals. The underlying mechanisms in the signal reduction for these two methods are also presented. For presaturation the signal reduction is due to the strong interaction between water and membrane lipid. Saturation of the water resonance using weak radio frequency (r.f.) irradiation of 2–5 s allows transfer of the lipid magnetization to the water resonance through the nuclear overhauser effect (NOE). However, with the selective gradient echo methods the magnetizations of all resonances are on the transverse plane for the majority of the selective echo time and thus subject to transverse relaxation decay. This often results in significant decay of signals that have short transverse relaxation times. We propose to use a water suppression technique similar to CHESS [17], composed of three selective pulses and three pulsed gradients. In contrast to CHESS which always uses 90° selective pulses, we calibrate the third selective excitation to empirically null (SEEN) the water signal. This selective pulse of between 90 and 180° is essential with HR-MAS since the MAS modulation of field inhomogeneities reduces the spatial excitation of the selective pulse (vide infra). The SEEN water suppression technique is easy to use and we demonstrate its advantages in comparison to presaturation, excitation sculpting, CHESS, and WET [18,19] using surgically resected human sarcoma tissues and a malignant sarcoma cell line. Modification of the third selective pulse for CHESS was suggested to compensate for the short delay effects between two scans in MRI localized spectroscopy [20].

2. Experimental methods

2.1. Sample preparation

2.1.1. Tumors

All tumor specimens were received fresh after operative resection at Memorial Sloan-Kettering Cancer Center with patients consent. The tissue was cut into slivers and immersed in PBS solution (90% H_2O/10% D_2O, pH 7.4) for 2 min. Excess liquid was removed by blotting and the tissue was then loaded into the 4 mm OD zirconium NMR rotor. The sample weight averaged 39.0 ± 3.0 mg.

2.1.2. Cells

Malignant peripheral nerve sheath tumor (MPNST) cells were cultured in basic RPMI media supplemented with 15% fetal bovine serum and penicillin and streptomycin for 24 h at 37 °C and 5% CO_2, to 65% confluence. Approximately 1.5×10^7 cells were harvested and centrifuged at 400*g* for 6 min. The pellet was then washed twice in PBS solution (90% H_2O/10% D_2O, pH 7.4), and centrifuged at 500*g* for 5 min at 4 °C. The cells were then transferred to the rotor.

2.2. MAS NMR experiments

The experiments were carried out at 20 °C on a Bruker Avance 600 MHz spectrometer with a 4 mm HR-MAS probe. The MAS rate used was 5000 ± 2 Hz. The pulsed field gradients were applied at the magic angle (54.7 °C) and all the applied gradients were sine-shaped.

The water suppression sequence SEEN is shown in Fig. 1. The first two selective pulses are 90° and the third selective pulse is between 90 and 180°. The fourth pulse is a hard 90° pulse, which excites all the magnetization to the transverse plane for detection. The selective pulses used in our experiments are half Gaussian shape (utilizing its high selective excitation efficiency) and can be replaced with any shaped excitation pulse.

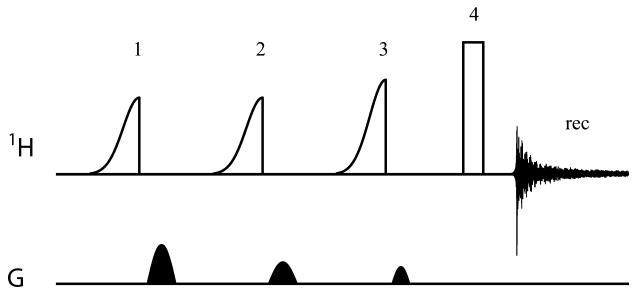

Fig. 1. The SEEN pulse sequence for water suppression. This pulse sequence includes three selective pulses and one hard detecting pulse with three pulsed gradients. The first two selective pulses are 90° and the third one needs to be empirically calibrated to achieve a null water signal. The fourth pulse is a hard 90° pulse for detection. The phases for the pulses are $\phi_1 = -x\ x\ x\ -x\ -y\ y\ y\ -y$; $\phi_2 = y\ y\ -y\ -y\ x\ x\ -x\ -x$; $\phi_3 = x\ -x\ y\ -y$; and $\phi_4 = \phi_{rec} = x\ -x\ -x\ x\ y\ -y\ -y\ y$.

The required intensities of the first two shaped pulses were calculated from the hard 90° pulse (e.g., using the Bruker shape tool STDISP), the third selective pulse is calibrated empirically until the water signal approaches zero. The approach for this calibration is similar to the 90° hard pulse calibration. The length of each selective 90° pulses used in the experiments is 10 ms. The three pulsed gradients used were 1 ms × 0.19 T/m, 1 ms × 0.055 T/m, and 0.5 ms × 0.085 T/m, respectively.

Presaturation was achieved using 2 s weak r.f. irradiation with an intensity of approximately 700 Hz. In the excitation sculpting approach, the two selective pulses were 4.4 ms Gaussian truncated at 1%, the first two gradients were 1 ms × 18 g/cm and the second two gradients were 1 ms × 10.3 g/cm. All the selective pulses used in CHESS and WET were 10 ms half Gaussian and the pulsed gradients were 1 ms × 0.48 T/m, 1 ms × 0.24 T/m, 1 ms × 0.12 T/m, and 1 ms × 0.06 T/m, respectively.

Total acquisition time was approximately 24 min for all experiments using 128 scans and an inter-scan delay of 10 s except in the case of presaturation, where the sum of presaturation and inter-scan delay was 10 s (so as to use the same overall acquisition time). The data sizes in the time domain and the frequency domain were 16 K for all the experiments. No line-broadening was applied for any experiments.

The 2D NOESY spectra were acquired without water suppression. To prevent radiation damping, gradients were applied during the evolution period and the mixing period [21]. The parameters used for the acquisition of the NOESY spectra include: 16 dummy scans; eight scans for each FID; data size, 512 × 2048 in the

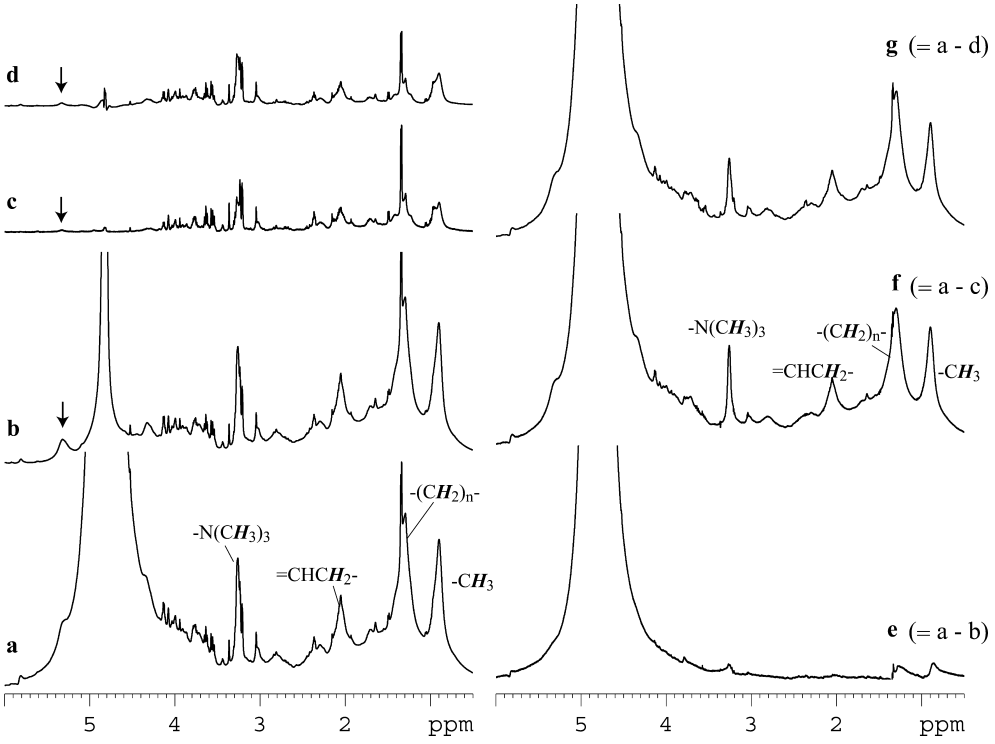

Fig. 2. MAS spectra of a gastrointestinal stromal tumor (GIST) freshly resected from a patient: a, acquired using a 90° pulse; b, acquired using the pulse sequence SEEN as shown in Fig. 1. The four pulsed field gradients were G_1: 1 ms × 0.19 T/m, G_2: 1 ms × 0.085 T/m, G_3: 1 ms × 0.055 T/m, G_4, 0.5 ms × 0.085 T/m; c, acquired using presaturation to suppress water; d, acquired using excitation sculpting [16] to suppress water. e–g are the difference spectra of a and b, a and c, and a and d, respectively. All the spectra are shown at the same scale. a–d were acquired and processed using the same parameter settings.

time domain, 2048×2048 in the frequency domain. Cosine window function was applied for both dimensions prior to Fourier transformation. Baseline correction was also applied in both dimensions.

3. Results and discussion

3.1. Comparison of SEEN with presaturation and excitation sculpting

Fig. 2 shows the proton MAS spectra of a fresh gastrointestinal stromal tumor (GIST) tissue sample and Fig. 3 shows the proton MAS spectra of an MPNST cell line: a, using a 90° pulse; b, using SEEN; c, using presaturation; d, using excitation sculpting; e, f, and g are the difference spectra of a and b, a and c, and a and d, respectively. All the spectra were acquired using the same receiver gain and are represented on the same scale. A brief assignment is shown in spectra 2a and 2f.

Both presaturation and excitation sculpting achieve almost complete water suppression and a very flat baseline as seen in spectra c and d in Figs. 2 and 3. They both, however, resulted in significant signal loss, especially for the lipid resonances when compared to spectra acquired without the use of water suppression (spectra 2a and 3a). The difference spectra f and g in Figs. 2 and 3 reveal the quantitative differences in spectral intensity between spectra acquired with no water suppression and spectra acquired with presaturation (f) or spectra acquired with excitation sculpting (g) and shows that the loss in signal intensity is due to a reduction in pure lipid resonances. In the presaturation spectra (f) of GIST tissue and MPNST cells the resonance at 0.93 ppm arising from the terminal methyl group of phospholipid hydrocarbon chains was reduced by 75 and 73%, respectively, compared to the spectra acquired without water suppression. In the excitation sculpting spectra (g) of GIST tissue and MPNST cells the resonance at 0.93 ppm was reduced by 79 and 74%, respectively, compared to spectra acquired without water suppression. The quantitative difference spectra Figs. 2e and 3e demonstrate that no significant signal intensity change occurs with SEEN.

Although the signal loss for the presaturation and selective gradient echo pulse sequences are approximately equal (~75% for the methyl on hydrocarbon chain lipid), the mechanisms are different. There was strong NOE interaction between water and membrane lipids observed in different tissues and cell lines (see

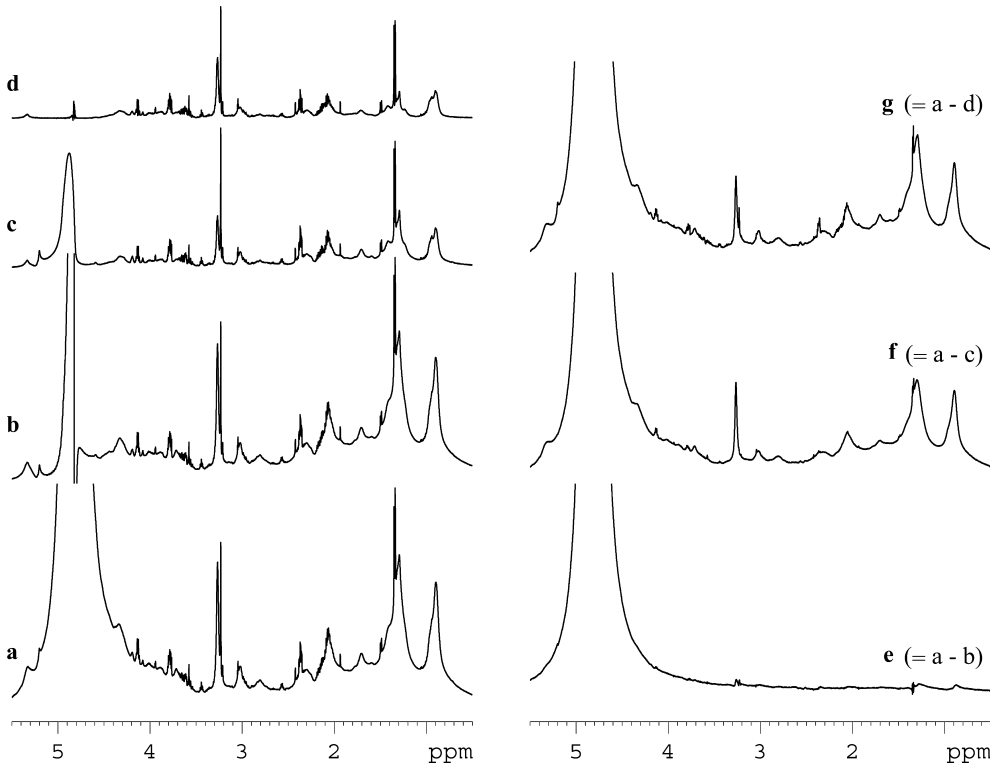

Fig. 3. MAS spectra of 1.5×10^7 human malignant peripheral nerve sheath tumor (MPNST) cells: a, acquired using a 90° pulse; b, acquired using the pulse sequence SEEN as shown in Fig. 1. The four pulsed field gradients were G_1: 1 ms × 0.19 T/m, G_2: 1 ms × 0.085 T/m, G_3: 1 ms × 0.055 T/m, G_4: 0.5 ms × 0.085 T/m; c, acquired using presaturation to suppress water; d, acquired using Excitation Sculpting to suppress water. e–g are the difference spectra of a and b, a and c, and a and d, respectively. All the spectra are shown at the same scale. a–d were acquired and processed using the same parameter settings.

below). In the case of presaturation, a 2–5 s irradiation time of the water peak with a weak r.f. pulse is normally required to achieve adequate water suppression. During this irradiation period, the lipid-magnetization is transferred to water through NOE. The loss of lipid signals in Figs. 2f and 3f represents the net magnetization transfer from lipid membrane protons to water during the irradiation period. The fraction of signal loss in presaturation depends on the time of the irradiation. Prior to saturation of the spin system, longer irradiation always reduces more of the lipid signals. In contrast, the decay of the lipid signals in the excitation sculpting experiments was due to the short transverse relaxation time of the lipids resonances. The magnetizations were on the transverse plane for the majority of the selective gradient echo time and the transverse relaxation time of the lipid resonances are only a few milliseconds. In the experiment, the overall time of two selective gradient echoes was about 9 ms. A detailed calculation of the magnetization decay is complicated because during the selective pulse, part of the magnetization is also in the longitudinal direction. Under MAS, the delay between two pulses should be carefully chosen in concert with the spin rate (the period), i.e., integer times of the period. The WATERGATE [22,23] experiment which does not use a soft selective pulse but uses the combination of hard pulses to achieve selective refocusing of water is not considered here. Under MAS, the delay between two hard pulses must be integer times of the period. This only allows a very fast MAS rate. For example, a 5000 Hz excitation band between two nulls for WATERGATE will need a MAS rate of 10 kHz. We have found that at spin rates of 5–6 kHz which is optimal for cell and tissue preservation that the use of WATERGATE for water suppression results in a twisting artifact in the spectra. The subtraction errors in Figs. 2e and 3e are from eddy current generated by the pulsed gradient. This was confirmed by demonstrating no subtraction error when SEEN is applied without using pulsed gradients (data not shown). The gradient coil used in the high-resolution MAS NMR probe is unshielded and using a shielded gradient coil should significantly reduce these errors.

The residual water resonance is substantially higher with the SEEN technique of water suppression compared to either presaturation or excitation sculpting methods. However, the SEEN sequence permits enough water suppression to avoid dynamic range problems and at the same time preserves the intensity of the lipid resonances enabling quantitative measurement of all proton spectral resonances. The vinyl peak at 5.4 ppm (shown by the arrows) is cleanly isolated from the water peak and its intensity is preserved when the SEEN water suppression sequence is applied (see spectra in Figs. 2b and 3b). In contrast, this vinyl resonance overlaps substantially with the water resonance in the absence of water suppression (see spectra in Figs. 2a and 3a). Although the presaturation and excitation sculpting methods remove the overlap of the vinyl peak and the water resonance, they both dramatically reduce the intensity of this resonance. It is important to clearly visualize and quantitate this vinyl resonance since it can be used to characterize the saturation of the fatty acid chains of the membrane lipids in intact cells and tissue specimens. Examination of these spectra reveal that the baseline is straighter with less undulation in the spectra acquired with presaturation and excitation sculpting compared to those acquired with SEEN. The very broad peaks detected in SEEN spectra represent the more bound metabolites in the cells and tissues, such as non-mobile membrane and protein signals. Apparently these broad peaks also undergo interaction with water through NOE or relayed NOE and are thus largely removed from spectra acquired with presaturation and excitation sculpting.

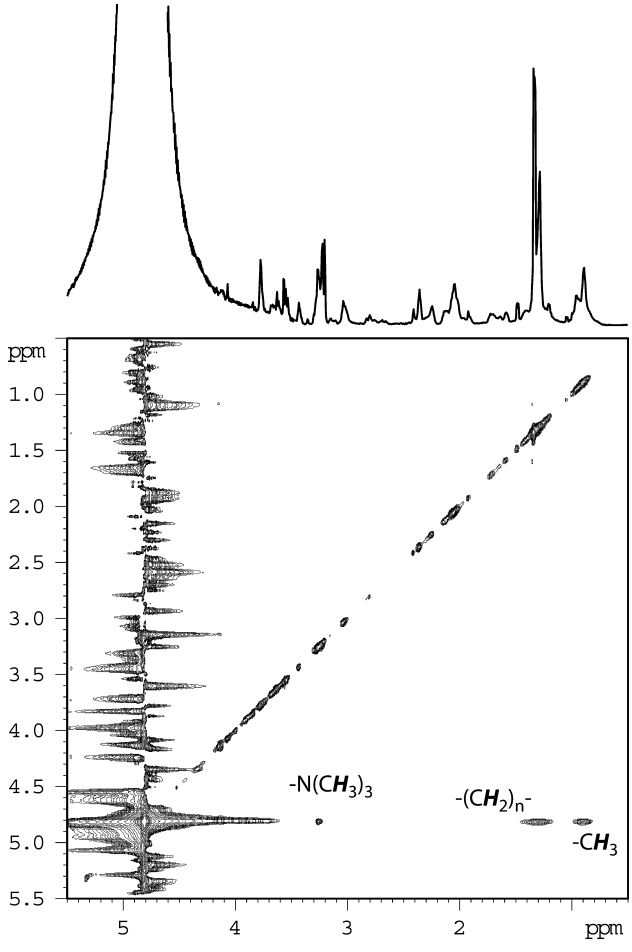

Fig. 4. 2D NOESY spectrum acquired using a fresh GIST tumor with the mixing time of 150 ms. The top 1D spectrum is the projection of the 2D NOESY spectrum. The dominant cross peaks are between water and the membrane associated lipids. The remaining cross peaks are weak and at a level just below the noise.

3.2. Two-dimensional NOESY shows the strong NOEs between water and lipid signals

To illustrate the existence of NOE between water and lipid signals a 2D NOESY spectrum is shown in Fig. 4 using a fresh GIST sample with the mixing time of 150 ms. On the top of the NOESY is the 1D projection of the 2D spectrum. The only cross peaks apparent in this spectrum are the NOEs between water and the lipid membrane. This NOESY was acquired without water suppression to observe the NOEs from water. The other NOEs are too low to be detectable in this NOESY because a low receiver gain is used to retain the strong water signal. This strong water–lipid NOE suggests that a significant number of water molecules are in close association with lipids in membrane bilayers of both cells and tissue samples. A detailed quantitative analysis and discussion of water–lipid NOE will be published elsewhere.

3.3. Comparison of SEEN with CHESS and WET

For water suppression, CHESS and WET do not result in lipid signal loss as is seen in presaturation or excitation sculpting since they use the same mechanism as SEEN. In these sequences, the selective pulses are on the order of 10 ms so that the magnetization transfer from lipids to non-equilibrium water is negligible. Also, the remaining resonances are at equilibrium during selective excitation of water, which prevents the fast decay by transverse relaxation that can be seen with excitation sculpting. However, we found that CHESS always results in a positive water signal while WET has a fairly broad suppression band. In Fig. 5, the water suppression profiles for SEEN (a), CHESS (b), and WET (c) are presented. At on-resonance, both SEEN and WET achieve good water suppression with the residual water signals in a dispersive shape. The dashed line in Fig. 5 is the same in all three profiles and identifies the difference in the suppression band. SEEN and CHESS have narrower offset effects compared to WET. It is clear that the suppression band for WET is the broadest. Due to radiation damping, the difference of the excitation profile shown in Fig. 5 has a much more significant effect on the area of the spectral signal than is readily apparent from intensity measurements (about the radiation damping effects in the water profile, see [23]). WET reduces signal intensity 3% at a distance of 700 Hz to water. We also found the vinyl resonance at 5.33 ppm has 10% less intensity when using WET to suppress water than using SEEN. However, when the signal close to water is not important in experiments, both methods are considered to be similar.

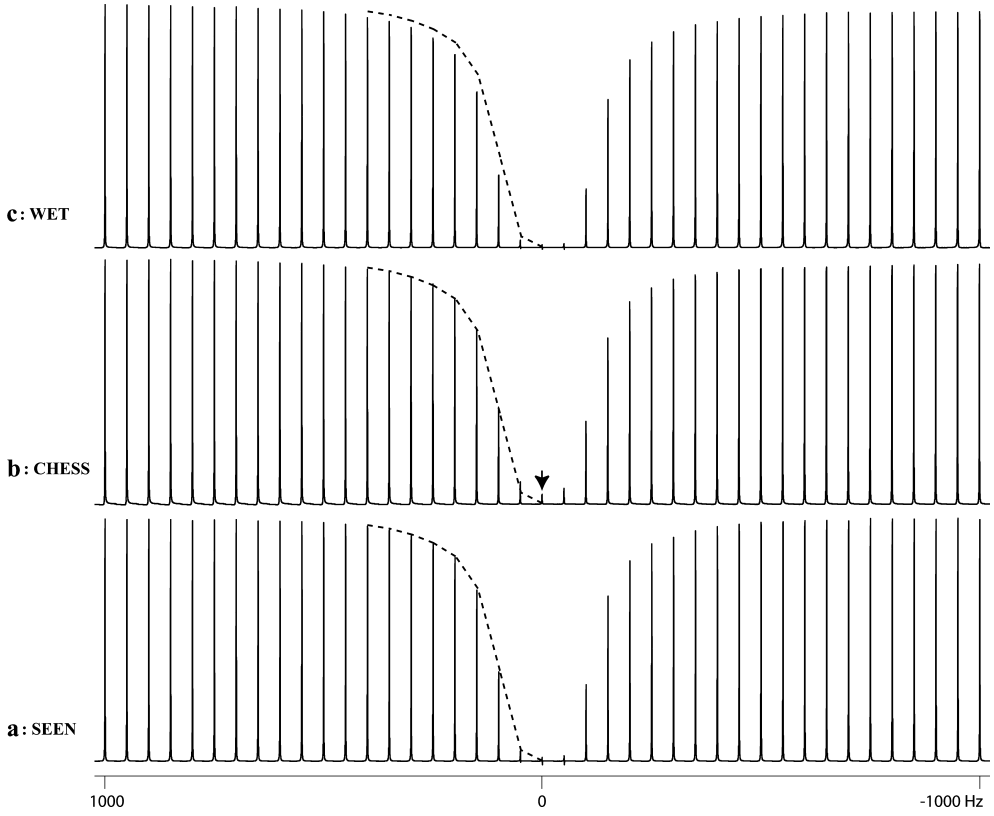

Fig. 5. Comparison of the suppression profiles of SEEN, CHESS and WET. CHESS leaves a positive water signal with an intensity that is 4% of the water resonance intensity in the absence of water suppression. WET has a broad suppression band.

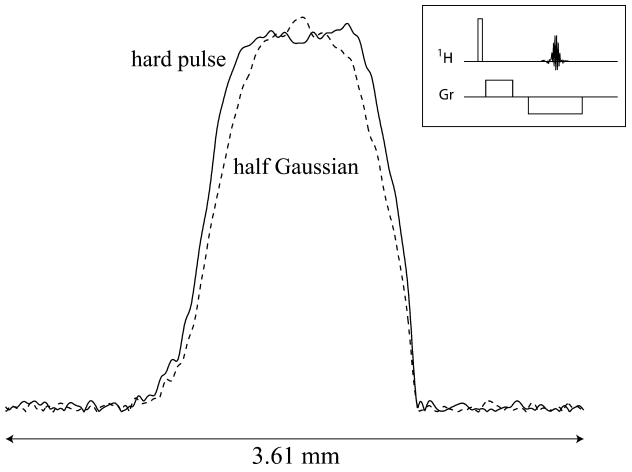

Fig. 6. Space excitation profile of a hard 90° pulse (the outside solid curve) and of a half Gaussian 90° pulse (the inside dashed curve) for a high-resolution MAS NMR probe at 600 MHz. It is apparent that the hard pulse is spaciously more efficient. The hard pulse excites part of longitudinal magnetization to the transverse plane. In contrast, the selective pulse (a half Gaussian) does not alter the longitudinal magnetization and leaves a positive water signal as is seen with CHESS water suppression. The inset shows the gradient echo sequence used to acquire the space profile on a sample of 1% H_2O with 99% D_2O. It is worth noting that using a sample with a higher concentration of H_2O results in radiation damping effects and complicates the profile.

CHESS leaves the residual water signal in an absorptive shape with an intensity of approximately 4% of the original intensity without water suppression (see the on-resonance signal). This residual signal comes from the fact that the space excitation profile of the selective pulse is narrower than the hard pulse. Fig. 6 shows the space excitation profile of a hard 90° pulse (the outside solid curve) and of a half Gaussian 90° pulse (the inside dashed curve). The hard pulse excites part of longitudinal magnetization to the transverse plane. In contrast, the selective pulse (a half Gaussian) does not alter the longitudinal magnetization and leaves a positive water signal as is seen with CHESS water suppression. The underlying physics is such that at the ends of the rotor, the field inhomogeneities are larger and the spins see a modulated B_z field from MAS. Since the selective pulse is of lower amplitude it is less able to compete with this modulation and it is inefficient at the ends of the rotor. The positive water signal in CHESS results from the magnetization at the edge of the excitation profile that cannot be excited by the selective pulse but that is excited by the hard 90° pulse. The longer pulse width in SEEN simply corresponds to a nulling signal from the residual z-magnetization at the ends of the rotor with a little inverted z-magnetization from the sample in the center of the rotor.

4. Conclusion

We have shown that solvent suppression using conventional presaturation and selective gradient echo methods for the study of tissue specimens and cultured cell lines result in more than a 70% reduction in the intensities of lipid resonances. The combination of selective excitation and pulsed gradients for water suppression avoids the signal loss found with conventional presaturation and selective gradient echo methods. The sequence proposed here (SEEN) achieves good water suppression and a fairly narrow suppression band.

Acknowledgments

The authors thank Murray F. Brennan for all his support and help in enabling this work. This manuscript was supported in part by the Kristen Ann Carr Fund and the Department of Surgery at MSKCC. J.H. Chen thanks Dr. Alexej Jerschow for helpful discussions.

References

[1] E.R. Andrew, A. Bradbury, R.G. Eades, Removal of dipolar broadening of NMR spectra of solids by specimen rotation, Nature 183 (1959) 1802–1803.
[2] L.L. Cheng, M.J. Ma, L. Becerra, T. Ptak, I. Tracey, A. Lackner, R.G. Gonzalez, Quantitative neuropathology by high resolution magic angle spinning proton magnetic resonance spectroscopy, Proc. Natl. Acad. Sci. USA 94 (1997) 6408–6413.
[3] J.H. Chen, B.M. Enloe, P. Weybright, N. Campbell, D. Dorfman, C.D. Fletcher, D.G. Cory, S. Singer, Biochemical correlates of thiazolidinedione-induced adipocyte differentiation by high-resolution magic angle spinning NMR spectroscopy, Magn. Reson. Med. 48 (2002) 602–610.
[4] J.L. Griffin, J.C. Pole, J.K. Nicholson, P.L. Carmichael, Cellular environment of metabolites and a metabonomic study of tamoxifen in endometrial cells using gradient high resolution magic angle spinning 1H NMR spectroscopy, Biochim. Biophys. Acta 1619 (2003) 151–158.
[5] J.Z. Hu, R.A. Wind, Sensitivity-enhanced phase-corrected ultra-slow magic angle turning using multiple-echo data acquisition, J. Magn. Reson. 163 (2003) 149–162.
[6] M.E. Bollard, S. Garrod, E. Holmes, J.C. Lindon, E. Humpfer, M. Spraul, J.K. Nicholson, High-resolution (1)H and (1)H–(13)C magic angle spinning NMR spectroscopy of rat liver, Magn. Reson. Med. 44 (2000) 201–207.
[7] S. Garrod, E. Humpfer, M. Spraul, S.C. Connor, S. Polley, J. Connelly, J.C. Lindon, J.K. Nicholson, E. Holmes, High-resolution magic angle spinning 1H NMR spectroscopic studies on intact rat renal cortex and medulla, Magn. Reson. Med. 41 (1999) 1108–1118.
[8] K. Millis, P. Weybright, N. Campbell, J.A. Fletcher, C.D. Fletcher, D.G. Cory, S. Singer, Classification of human liposarcoma and lipoma using ex vivo proton NMR spectroscopy, Magn. Reson. Med. 41 (1999) 257–267.
[9] Y. Perez, H. Lahrech, M.E. Cabanas, R. Barnadas, M. Sabes, C. Remy, C. Arus, Measurement by nuclear magnetic resonance diffusion of the dimensions of the mobile lipid compartment in C6 cells, Cancer Res. 62 (2002) 5672–5677.
[10] B. Sitter, U. Sonnewald, M. Spraul, H.E. Fjösne, I.S. Gribbestad, High-resolution magic angle spinning MRS of breast cancer tissue, NMR Biomed. 15 (2002) 327–337.
[11] J.H. Chen, B.M. Enloe, C.D. Fletcher, D.G. Cory, S. Singer, Biochemical analysis using high-resolution magic angle spinning

NMR spectroscopy distinguishes lipoma-like well-differentiated liposarcoma from normal fat, J. Am. Chem. Soc. 123 (2001) 9200–9201.

[12] D. Moka, R. Vorreuther, H. Schicha, M. Spraul, E. Humpfer, M. Lipinski, P.J. Foxall, J.K. Nicholson, J.C. Lindon, Biochemical classification of kidney carcinoma biopsy samples using magic-angle-spinning 1H nuclear magnetic resonance spectroscopy, J. Pharm. Biomed. Anal. 17 (1998) 125–132.

[13] D.I. Hoult, Solvent peak saturation with single phase and quadrature Fourier transformation, J. Magn. Reson 21 (1976) 337–347.

[14] M.C. Martinez-Bisbal, L. Marti-Bonmati, J. Piquer, A. Revert, P. Ferrer, J.L. Llacer, M. Piotto, O. Assemat, B. Celda, 1H and (13)C HR-MAS spectroscopy of intact biopsy samples ex vivo and in vivo (1)H MRS study of human high grade gliomas, NMR Biomed. 17 (2004) 191–205.

[15] M. Piotto, V. Saudek, V. Sklenár, Gradient tailored excitation for single quantum spectroscopy of aqueous solutions, J. Biomol. NMR 2 (1992) 661–665.

[16] T. Hwang, A.J. Shaka, Water suppression that works. Excitation sculpting using arbitrary waveforms and pulsed field gradients, J. Magn. Reson. A 112 (1995) 275–279.

[17] A. Haase, J. Frahm, W. Hanicke, D. Matthaei, 1H NMR chemical shift selective (CHESS) imaging, Phys. Med. Biol. 30 (1985) 341–344.

[18] R.J. Ogg, P.B. Kingsley, J.S. Taylor, WET, a T1- and B1-insensitive water-suppression method for in vivo localized 1H NMR spectroscopy, J. Magn. Reson. B 104 (1994) 1–10.

[19] S.H. Smallcombe, S.L. Patt, P.A. Keifer, WET solvent suppression and its application to LC NMR and high-resolution NMR spectroscopy, J. Magn. Reson. A 117 (1995) 295–303.

[20] P.G. Webb, N. Sailasuta, S.J. Kohler, T. Raidy, R.A. Moats, R.E. Hurd, Automated single-voxel proton MRS: technical development and multisite verification, Magn. Reson. Med. 31 (1994) 365–373.

[21] B. Cutting, J.H. Chen, D. Moskau, G. Bodenhausen, Radiation damping compensation of selective pulses in water–protein exchange spectroscopy, J. Biomol. NMR 17 (2000) 323–330.

[22] V. Sklenar, M. Piotto, R. Leppik, V. Saudek, Gradient-tailored water suppression for 1H-15N HSQC experiments optimized to retain full sensitivity, J. Magn. Reson. A 102 (1993) 241–245.

[23] M. Liu, X.A. Mao, C. Ye, H. Huang, J.K. Nicholson, J.C. Lindon, Improved WATERGATE pulse sequences for solvent suppression in NMR spectroscopy, J. Magn. Reson 132 (1998) 125–129.